Published in final edited form as:
Mech Dev. 2011 ; 128(0): 200–207. doi:10.1016/j.mod.2010.12.002.

Dicer activity in neural crest cells is essential for craniofacial organogenesis and pharyngeal arch artery morphogenesis

Xuguang Nie[a,1], **Qin Wang**[b], and **Kai Jiao**[a,*]

[a]Department of Genetics, University of Alabama at Birmingham, Birmingham, AL 35294, USA

[b]Department of Physiology and Biophysics, University of Alabama at Birmingham, Birmingham, AL 35294, USA

Abstract

MicroRNAs (miRNAs) play important roles in regulating gene expression during numerous biological/pathological processes. *Dicer* encodes an RNase III endonuclease that is essential for generating most, if not all, functional miRNAs. In this work, we applied a conditional gene inactivation approach to examine the function of *Dicer* during neural crest cell (NCC) development. Mice with NCC-specific inactivation of *Dicer* died perinatally. Cranial and cardiac NCC migration into target tissues was not affected by *Dicer* disruption, but their subsequent development was disturbed. NCC derivatives and their associated mesoderm-derived cells displayed massive apoptosis, leading to severe abnormalities during craniofacial morphogenesis and organogenesis. In addition, the 4th pharyngeal arch artery (PAA) remodeling was affected, resulting in interrupted aortic arch artery type B (IAA-B) in mutant animals. Taken together, our results show that *Dicer* activity in NCCs is essential for craniofacial development and pharyngeal arch artery morphogenesis.

Keywords

Neural crest cells; Craniofacial; Aortic arch artery; *Dicer*

1. Introduction

Neural crest cells (NCCs) are multipotent stem cells that are generated at the interface between the non-neural ectoderm and neural tube along the neuroaxis. Shortly after generation, NCCs migrate ventrally from the neural tube to target embryonic areas where they are differentiated into various cell types such as osteogenic and chondrogenic cells, neural and glial cells, and vascular smooth muscle cells (Graham et al., 2004). NCCs that migrate to the facial primordia are known as cranial NCCs and they form most of the craniofacial skeleton. NCCs that migrate to the cardiac region are known as cardiac NCCs. Cardiac NCCs migrate to the pharyngeal arch arteries (PAAs) and cardiac outflow tract

*Corresponding author. Tel.: +1 205 996 4198; fax: +1 205 975 5689. kjiao@uab.edu (K. Jiao).
[1]Present address: Department of Genetics and Genomic Sciences, Mount Sinai School of Medicine, 1425 Madison Avenue, New York, NY 10029, USA.

(OFT) through pharyngeal arch (PA) 3–6, forming smooth muscle cells of great vessels and participating in PAA and OFT remodeling (Brown and Baldwin, 2006; Hutson and Kirby, 2007; Snider et al., 2007; Stoller and Epstein, 2005). Defective NCC development accounts for many human congenital abnormalities involving craniofacial and cardiovascular structures (OMIM, 192430; 148820).

MiRNAs are evolutionally conserved small RNA molecules that act on the 3′ untranslated region of target mRNAs to downregulate their stability and translation efficiency (Cordes and Srivastava, 2009; Fabian et al., 2010; Liu and Olson, 2010; Wang, 2010; Zhao and Srivastava, 2007). Genes encoding miRNAs are transcribed by RNA polymerase II or III to generate Pri-miRNAs, which are processed to Pre-miRNAs by Drosha in the nucleus. Pre-miRNAs are exported to the cytoplasm where they are further processed by the RNase III ribonuclease *Dicer* to generate ~22 nucleotide single strand mature miRNAs (Cordes and Srivastava, 2009; Fabian et al., 2010; Liu and Olson, 2010; Wang, 2010; Zhao and Srivastava, 2007). Therefore *Dicer* is required for generation of most, if not all, functional miRNAs. Tissue specific inactivation of *Dicer* reveals important roles for *Dicer* in the development of a number of organs and tissues, such as the brain, heart, eye, muscle and skeleton (Chen et al., 2008; Huang et al., 2010a,b; Kobayashi et al., 2008; Li and Piatigorsky, 2009; O'Rourke et al., 2007; Saxena and Tabin, 2010; Zehir et al., 2010).

In this work, we analyzed craniofacial organogenesis and pharyngeal arch artery remodeling in mice in which *Dicer* was specifically inactivated in NCCs. NCC-disruption caused NCC survival defects, which further led to neighboring mesoderm mesenchymal cell death. This abnormal cell death caused severe abnormalities in craniofacial morphogenesis and organogenesis. In addition, we show that *Dicer* is required for normal remodeling of the 4th PAA. Our results, in combination with three recent studies applying a similar conditional gene inactivation approach (Huang et al., 2010a,b; Zehir et al., 2010), collectively establish the critical role of *Dicer* in NCCs to regulate development of craniofacial structures, the neural system and the cardiovascular system.

2. Results

2.1. Defective oro-craniofacial morphogenesis in mutant mice

To study the function of *Dicer* during NCC development, we crossed *Wnt1-Cre* mice (Danielian et al., 1998) with $Dicer^{loxP/loxP}$ (Cobb et al., 2005) mice to acquire male *Wnt1-Cre*; $Dicer^{loxP/+}$ mice, which were then crossed with female $Dicer^{loxP/loxP}$ mice to acquire mutant animals (*Wnt1-Cre*; $Dicer^{loxP/loxP}$). Mutant mice died perinatally. No gross abnormality was observed in mutants until E11.5. Starting from E12.5, the mutant embryos were recognizable by retrognathia faces (Fig. 1A and B). A tiny head became obvious in mutants at later developmental stages (Fig. 1C and D). At the newborn stage, mutants showed clear craniofacial abnormalities, including microcephaly, facial hypoplasia, short nose, microstomia, complete cleft palate and open eyelids (Fig. 1E–H).

Histological examination revealed that mutant embryos started to display abnormal morphogenesis as early as E11.5 (Fig. 1I and J). At this stage, expansion of bilateral lingual swellings was delayed in mutants. At E13.5, the tongue bud was obviously smaller than that

observed in controls. The palatal shelves of the mutant embryos, although sprouted, were rudimentary and did not display obvious vertical outgrowth as in controls (Fig. 1K and L). Palatal shelf development was arrested before reaching the midline, leading to bilateral complete palatal cleft in all mutants examined (Fig. 1M and N).

2.2. Defects in craniofacial skeletogenesis and muscle development in mutant mice

Craniofacial skeletons are mostly formed by NCCs except the parietal and occipital bones, which are formed by cells from paraxial mesoderm. Histological examinations revealed that skeletons such as Meckel's cartilage were not formed in mutant embryos (Fig. 1K–N), consistent with previous reports (Huang et al., 2010a; Zehir et al., 2010). Skeletal staining with Alizarin red and Alcian blue in newborn animals showed that the craniofacial skeletons were either missing or rudimentary (Fig. 2A–D).

We further examined the development of cartilaginous structures using the chondrogenic marker *Sox9* at stage E13.5, when precursors for craniofacial cartilage have normally been formed. At this stage, high expression of *Sox9* was detected in the developing Meckel's cartilage in the mandibular arch of controls, but was absent in mutants (Fig. 2E and F). Also, by this stage, formation of the cartilaginous chondrocranium was evident in controls, but was incomplete in mutants, as indicated by *Sox9* expression (Fig. 2E and F). A closer examination showed that precursors of the sphenoid bone were only rudimentary and precursors for the ethmoid bone were undetectable; nevertheless, precursors for the basioccipital bone appeared normal (Fig. 2E and F). Thus, NCC-derived anterior basicranium was largely missing.

We continued to determine if early osteogenic differentiation was affected in the mutant embryos by examining *Cbfa1* expression. *Cbfa1* is a specific marker for osteogenic cells (Ducy et al., 1997). We detected a number of *Cbfa1* expressing cells aggregated within the maxillary arch of the mutant embryos at E12.5 (Fig. 2G and H). However, the *Cbfa1*-expressing cells were visibly disorganized compared to controls, and were absence from many sites such as the distal mandibular arch (Fig. 2G and H). Collectively, these data suggest that chondrogenesis and osteogenesis are severely disturbed in mutant mice.

Craniofacial muscles are derived from cranial and somite mesenchymal cells. Their proper development requires continuous communication with NCCs (Noden and Francis-West, 2006; Noden and Trainor, 2005; Rinon et al., 2007). We therefore examined muscle development in mutants using a myogenic differentiation marker, *MyoD*. We focused on the primitive tongue area, which is enriched with muscle precursor cells. In a control embryo at E13.5, cells expressing *MyoD* were organized in a striped pattern in the primitive tongue. While *MyoD* positive cells were clearly detected in the primitive tongue area of mutant embryos, no apparent organization could be observed among these cells, suggesting that craniofacial muscles were distorted in mutant tongues (Fig. 2I and J). Therefore, NCC-expression of *Dicer* is required for normal organization of muscle precursor cells.

2.3. Defective morphogenesis of cranial ganglion and nerves in mutant mice

NCCs play important roles in craniofacial structure innervation by directly forming neurons and glial cells in the cranial ganglia. We performed whole mount immunostaining using a 2H3 antibody to examine the development of the cranial ganglia and nerves in mutant embryos. At E10.5, trigeminal ganglia were clearly formed in the mutant and were morphologically comparable to the controls. However, the size of mutant trigeminal ganglia appeared to be slightly reduced compared to that of controls (Fig. 3A and B), and this slight reduction in size has been repeatedly observed in multiple embryos. By E11.5, we found that the mutant mandibular arch was visibly devoid of neural fibers (Fig. 3C and D), suggesting that neural axial navigation into the mandibular arch was impaired.

2.4. Dicer disruption in NCCs causes abnormal cell death, but has little effect on cell proliferation

We next tested whether abnormal cell proliferation and/or apoptosis contribute to the defect observed in mutants. We first performed proliferation assays using an anti-phospho Histone H3 antibody. We found that proliferating cells were widespread in the developing craniofacial tissues in both mutants and controls, and proliferation rates of both genotypes were comparable at two critical stages (E11.5 and E13.5), as shown in Fig. 4A–D. Similar results were obtained at multiple sectional planes. Therefore, we conclude that NCC-disruption of *Dicer* does not cause a cell proliferation defect. We then examined cell death by TUNEL. Our results showed markedly increased cell death within the facial primordia of the mutant mice beginning at E10.5, most notably in the mandibular arches at this stage (Fig. 5A–D). To test whether cell death was restricted to NCC-derived cells, we crossed *Wnt1-Cre*; $Dicer^{loxP/+}$ mice with $Dicer^{loxP/loxP}$; *R26R* mice. NCC derivative cells could thus be labeled by lacZ staining. Significantly, apoptosis was not limited to NCC-derived ectomesenchymal cells (lacZ positive), but was also found in mesoderm-derived mesenchymal cells (Fig. 5A–D). Increased cell death was also found in later developmental stages in the primitive tongue (Fig. 5E–H). Taken together, we conclude that increased apoptosis contributes significantly to defective craniofacial development.

2.5. Disruption of Dicer in NCCs does not affect NCC migration

Next, we sought to determine if NCC migration to the presumptive facial primordia and pharyngeal arches was affected by *Dicer* disruption. We examined expression of NCC migration markers *Ap-2* and *Crabp1* at E9.0, when NCCs populate within their migration paths and arches. *Ap-2* was highly expressed in NCCs along their migration paths within the PAs and in the presumptive craniofacial region. No difference in *Ap-2* expression was detected between mutants and controls (Fig. 6A and B). Similarly, expression of *Crabp1* in mutant embryos was also comparable to the control embryos (Fig. 6C and D). We further examined NCC migration using R26R mice. We did not observe obvious differences in the lacZ expression pattern between control and mutant embryos at E9.0 (Fig. 6E and F). We therefore conclude that the initial NCC migration was grossly normal in mutants.

2.6. Dicer activity in NCCs is critical for PAA morphogenesis

Cardiac NCCs are critical for PAA and OFT remodeling. PAAs are bilaterally symmetric until E11.5 and shortly, they undergo asymmetric remodeling. In *Wnt1-Cre*; *Dicer*$^{loxP/loxP}$ mice, the aortic arch (derived from the 4th PAA) appeared to be narrowed beginning at E12.5 (Fig. 7A and B), and the narrowed aortic arch defect became more apparent by E13.5 (Fig. 7C and D). Eventually, the aortic arch was disrupted, leading to interrupted aortic arch artery type B (IAA-B), which is a characteristic vascular defect observed in DiGeorge syndrome (DS) patients (Fig. 7E and F). NCCs play a critical role in separating the OFT into the aorta and pulmonary trunk. As such, maldevelopment of NCCs often causes an OFT separation defect (e.g. Nie et al., 2008). Intriguingly, no obvious defect was observed in the OFT of mutant embryonic hearts. Collectively, our results suggest that *Dicer* activity is required in NCCs for normal aortic arch development, but dispensable for OFT remodeling.

3. Discussion

Dicer encodes an RNase III ribonuclease critical for generation of functional miRNAs. Here we show that disruption of *Dicer* in NCCs causes a spectrumof defects during craniofacial development and PAA remodeling in mice. During preparation of this manuscript, three other groups published studies applying a similar conditional gene inactivation approach to determine the role of *Dicer* in NCCs (Huang et al.,2010a,b; Zehir et al., 2010). Our current study not only confirms and complements these studies, but also provides critical novel information regarding the function of *Dicer* during NCC development. Although craniofacial defects have been reported in all previous studies, we performed further molecular characterization of chondrogenesis and osteogenesis in mutant embryos by examining expression of *Sox9* and *Cbfa1* (Fig. 2A–H). In addition, we show, for the first time, that skeletal muscle cell organization was disrupted in mutant embryos, as revealed from the disorganized expression pattern of *MyoD* (Fig. 2I and J). Through cell lineage labeling, we show that increased cell death was not limited to NCCs, but was also observed in mesoderm-derived mesenchymal cells (Fig. 5), supporting the notion that continuous communication between NCCs and their surrounding cells is important for normal craniofacial and pharyngeal development. This piece of critical information is not included in previous reports. Moreover, these are the only studies in which both marker examination (*Crabp1*, *Ap-2*) and cell lineage analysis (Fig. 6) are performed to show that the morphological defects in mutants cannot be ascribed to abnormal migration of NCCs. Both our group and another (Huang et al., 2010b) have reported the IAA-B defect with 100% penetrance in mutant embryos. In our mouse model, no other cardiac defect was observed; whereas in the other study, all mutant embryos display the double-outlet-right-ventricle (DORV) defect (Huang et al., 2010b). We therefore provide a unique mouse model to characterize PAA remodeling defects without potential interference from abnormal OFT development. Some of these unique discoveries made by our study are further discussed below.

Wnt1-Cre inactivates target genes shortly after NCCs are formed (Danielian et al., 1998). Our data indicate that disruption of *Dicer* by *Wnt1-Cre* does not disturb NCC migration to facial primordia and pharyngeal arches. This result suggests that generation of functional

miRNAs in NCCs is not essential for NCC migration. However, we cannot exclude the possibility that sufficient functional miRNAs are retained in NCC derivatives to support their migration after deletion of the *Dicer* gene. We provide clear evidence showing that *Dicer* activities are required for normal survival of post-migratory NCC derivatives, which has also been observed by other groups (Huang et al., 2010a,b; Zehir et al., 2010). A unique and significant discovery of the current study is that abnormal cell death was observed not only in NCC derivatives, but also in mesoderm-derived mesenchymal cells. Recent studies have shown that NCCs secrete growth factors, which signal to surrounding cells to regulate their proper gene expression during craniofacial development (Rinon et al., 2007; Tzahor et al., 2003). Death of NCCs may reduce the total signal released from NCCs, causing cell death of surrounding non-NCC derivatives. Alternatively, *Dicer* may be required for normal expression of signaling molecules generated from NCCs to support survival and development of surrounding mesenchymal cells. Our results provide a strong piece of evidence supporting the notion that communication between NCCs and their surrounding cells is essential for normal craniofacial and pharyngeal morphogenesis.

Abnormal skeletogenesis in the craniofacial structure is a major defect caused by NCC disruption of *Dicer*. We showed that skeletal formation in mutants was severely affected at the condensation stage. At this stage, although a significant number of NCC derivatives were still present within the facial primordia of mutant embryos, these NCCs failed to form proper skeletal condensates. Consequently, mutant mice observed at term were missing most of their NCC- derived skeletons. This is particularly evident for chondrogenesis; condensates for NCC-derived cartilage were either absent or extremely small. This result is consistent with a recent study showing that *Dicer* is critical for chondrogenic cell differentiation and proliferation (Kobayashi et al., 2008).

Another significant defect in the craniofacial region of mutant embryos, which has not been reported by other groups, is the maldevelopment of muscles. We showed that although *MyoD* expressing cells could be clearly detected in the tongues of mutant embryos, these cells failed to organize into the striped pattern characteristic of control embryos (Fig. 2I and J). Similar results were observed in other facial areas (data not shown). Although myogenic cells are not directly derived from NCCs, NCC derivatives invade myogenic tissues to form connective tissues. Such invasion ensures continuous cell– cell communication between NCCs and muscle precursor cells and thus supports proper morphogenesis of craniofacial muscles (Noden and Francis-West, 2006; Rinon et al., 2007). Our data provide the first genetic evidence indicating that *Dicer* expressed in NCCs is required for normal organization of craniofacial muscle precursor cells.

Cardiac NCCs migrate to the pharyngeal and cardiac region to participate in PAA and OFT remodeling. Asymmetric PAA and OFT remodeling is regulated by complex mechanisms that remain to be elucidated. Our results showed that *Dicer* activities in NCCs are required for normal aortic arch artery morphogenesis. NCC-disruption of *Dicer* causes interruption of the aortic arch artery, resembling the IAA-B most often observed in DS patients (Emanuel et al., 2001; Momma et al., 1999; Ryan et al., 2001; Ryan and Chin, 2003). It was recently found that *DGCR8*, a gene within the commonly deleted genomic region in DS patients, encodes an essential component for Pri-miRNA processing (Gregory et al., 2004; Han et al.,

2004; Wang et al., 2007). Although it is still unclear whether heterozygosity of *DGCR8* contributes to pathological phenotypes in DS patients, our data clearly suggest that interfering with the formation of functional miRNAs by *Dicer* inactivation in NCCs leads to a DS-like PAA defect. It is intriguing to notice that *Dicer* is required in NCCs for normal PAA development, but dispensable for OFT remodeling in our study. In many published mouse models, maldevelopment of PAA is associated with abnormal OFT remodeling (e.g. Kaartinen et al., 2004; Liu et al., 2004; Nie et al., 2008). Our data suggest that PAA development is more sensitive to NCC-loss of *Dicer* than OFT development. Huang et al. (2010b) reported that in their study, all embryos with NCC-loss of *Dicer* displayed both IAA-B and DORV. We speculate that different results between the two studies are due to variations in mouse genetic backgrounds. Nevertheless, our study indicates that the PAA remodeling defect can occur independently of OFT abnormalities in mutant embryos, as observed in DS patients.

In conclusion, this study demonstrates that *Dicer* plays a critical role in supporting normal NCC development. These results will help us to better understand the mechanisms regulating NCC development in mammals.

4. Experimental procedures

4.1. Mouse maintenance, genotyping and tissue processing

All procedures were approved by the Institutional Animal Care and Use Committee at the University of Alabama at Birmingham. *Wnt1-Cre* mice (Danielian et al., 1998; purchased from The Jackson Laboratory) were crossed with $Dicer^{loxP/loxP}$ mice (Cobb et al., 2005) to generate *Wnt1-Cre*; $Dicer^{loxp/+}$ male mice, which were then crossed with $Dicer^{loxP/loxP}$ female mice to produce *Wnt1-Cre*; $Dicer^{loxP/loxP}$ mutant animals. Mouse genotypes were determined with PCR analysis using *Cre* and *Dicer* primers as described previously (Cobb et al., 2005; Danielian et al., 1998). For sectional analysis, all samples were fixed with 4% PFA, embedded and sectioned using routine procedures. For whole mount immunostaining and *in situ* hybridization analysis, the embryos were fixed with 4% PFA, and stored in 100% methanol at ~20 °C for further processing.

4.2. Skeletal preparation and staining with Alcian blue and Alizarin red

Skeleton preparation and staining with Alcian blue and Alizarin red was performed as previously described (Goodnough et al., 2007). Briefly, the heads of mice were fixed in 95% ethanol for 24 h, after which the skin and other soft tissues were removed from the skeleton. The head was then placed in acetone for 24 h to remove the fat, and was next stained with Alcian blue and Alizarin red solution for 3 days at room temperature. The stained skeleton was cleared with 1% KOH and stored in 80% glycerol.

4.3. Immunostaining and in situ hybridization

TUNEL staining was performed using DeadEnd Colorimetric TUNEL System (Promega) following the manufacture's protocol. For cell proliferation analysis, anti-phospho-Histone H3 polyclonal antibody (Upstate) was used to detect cells in M phase. Whole mount immunostaining for neurofilament was performed using a 2H3 anti-neurofilament

monoclonal antibody (Hybridoma Bank at the University of Iowa). Whole mount and non-radioactive sectional *in situ* hybridization was performed as previously described (Nie et al., 2008).

4.4. LacZ staining

LacZ staining was performed as previously described (Nie et al., 2008). Briefly, the embryos were fixed in 4% PFA at 4 °C for 1 h, washed in 1× PBS 3 times, and then stained in the dark with X-gal solution overnight at room temperature.

Acknowledgments

We thank Dr. M. Merkenschlager (MRC Clinical Sciences Centre, UK) for providing the *Dicer*$^{loxP/loxP}$ mouse line. We thank Drs. T. Williams, U. Colorado, Denver and D.Z. Wang, Children's Hospital Boston, Harvard Medical School, for providing *in situ* probes. We thank members of the Jiao laboratory for assistance on the project. This project is supported by grants from American Heart Association (0535177N and 09GRNT2060268) and UAB, HSF-GEF Scholar Award to Kai Jiao.

REFERENCES

Brown CB, Baldwin HS. Neural crest contribution to the cardiovascular system. Adv. Exp. Med. Biol. 2006; 589:134–154. [PubMed: 17076279]

Chen JF, Murchison EP, Tang R, Callis TE, Tatsuguchi M, Deng Z, Rojas M, Hammond SM, Schneider MD, Selzman CH, Meissner G, Patterson C, Hannon GJ, Wang DZ. Targeted deletion of Dicer in the heart leads to dilated cardiomyopathy and heart failure. Proc. Natl. Acad. Sci. USA. 2008; 105:2111–2116. [PubMed: 18256189]

Cobb BS, Nesterova TB, Thompson E, Hertweck A, O'Connor E, Godwin J, Wilson CB, Brockdorff N, Fisher AG, Smale ST, Merkenschlager M. T cell lineage choice and differentiation in the absence of the RNase III enzyme Dicer. J. Exp. Med. 2005; 201:1367–1373. [PubMed: 15867090]

Cordes KR, Srivastava D. MicroRNA regulation of cardiovascular development. Circ. Res. 2009; 104:724–732. [PubMed: 19325160]

Danielian PS, Muccino D, Rowitch DH, Michael SK, McMahon AP. Modification of gene activity in mouse embryos in utero by a tamoxifen-inducible form of *Cre* recombinase. Curr. Biol. 1998; 8:1323–1326. [PubMed: 9843687]

Ducy P, Zhang R, Geoffroy V, Ridall AL, Karsenty G. Osf2/Cbfa1: a transcriptional activator of osteoblast differentiation. Cell. 1997; 89:747–754. [PubMed: 9182762]

Emanuel BS, McDonald-McGinn D, Saitta SC, Zackai EH. The 22q11.2 deletion syndrome. Adv. Pediatr. 2001; 48:39–73. [PubMed: 11480765]

Fabian MR, Sonenberg N, Filipowicz W. Regulation of mRNA translation and stability by microRNAs. Annu. Rev. Biochem. 2010; 79:351–379. [PubMed: 20533884]

Goodnough LH, Brugmann SA, Hu D, Helms JA. Stage-dependent craniofacial defects resulting from Sprouty2 overexpression. Dev. Dyn. 2007; 236:1918–1928. [PubMed: 17576140]

Graham A, Begbie J, McGonnell I. Significance of the cranial neural crest. Dev. Dyn. 2004; 229:5–13. [PubMed: 14699573]

Gregory RI, Yan KP, Amuthan G, Chendrimada T, Doratotaj B, Cooch N, Shiekhattar R. The Microprocessor complex mediates the genesis of microRNAs. Nature. 2004; 432:235–240. [PubMed: 15531877]

Han J, Lee Y, Yeom KH, Kim YK, Jin H, Kim VN. The Drosha-DGCR8 complex in primary microRNA processing. Genes Dev. 2004; 18:3016–3027. [PubMed: 15574589]

Huang T, Liu Y, Huang M, Zhao X, Cheng L. Wnt1-Cre-mediated conditional loss of Dicer results in malformation of the midbrain and cerebellum and failure of neural crest and dopaminergic differentiation in mice. J. Mol. Cell. Biol. 2010a; 2:152–163. [PubMed: 20457670]

Huang ZP, Chen JF, Regan JN, Maguire CT, Tang RH, Rong Dong X, Majesky MW, Wang DZ. Loss of MicroRNAs in neural crest leads to cardiovascular syndromes resembling human congenital heart defects. Arterioscler. Thromb. Vasc. Biol. 2010b; 30:2575–2586. [PubMed: 20884876]

Hutson MR, Kirby ML. Model systems for the study of heart development and disease. Cardiac neural crest and conotruncal malformations. Semin. Cell Dev. Biol. 2007; 18:101–110. [PubMed: 17224285]

Kaartinen V, Dudas M, Nagy A, Sridurongrit S, Lu MM, Epstein JA. Cardiac outflow tract defects in mice lacking ALK2 in neural crest cells. Development. 2004; 131:3481–3490. [PubMed: 15226263]

Kobayashi T, Lu J, Cobb BS, Rodda SJ, McMahon AP, Schipani E, Merkenschlager M, Kronenberg HM. Dicer-dependent pathways regulate chondrocyte proliferation and differentiation. Proc. Natl. Acad. Sci. USA. 2008; 105:1949–1954. [PubMed: 18238902]

Li Y, Piatigorsky J. Targeted deletion of Dicer disrupts lens morphogenesis, corneal epithelium stratification, and whole eye development. Dev. Dyn. 2009; 238:2388–2400. [PubMed: 19681134]

Liu N, Olson EN. MicroRNA regulatory networks in cardiovascular development. Dev. Cell. 2010; 18:510–525. [PubMed: 20412767]

Liu W, Selever J, Wang D, Lu MF, Moses KA, Schwartz RJ, Martin JF. Bmp4 signaling is required for outflow-tract septation and branchial-arch artery remodeling. Proc. Natl. Acad. Sci. USA. 2004; 101:4489–4494. [PubMed: 15070745]

Momma K, Matsuoka R, Takao A. Aortic arch anomalies associated with chromosome 22q11 deletion (CATCH 22). Pediatr. Cardiol. 1999; 20:97–102. [PubMed: 9986884]

Nie X, Deng CX, Wang Q, Jiao K. Disruption of Smad4 in neural crest cells leads to mid-gestation death with pharyngeal arch, craniofacial and cardiac defects. Dev. Biol. 2008; 316:417–430. [PubMed: 18334251]

Noden DM, Francis-West P. The differentiation and morphogenesis of craniofacial muscles. Dev. Dyn. 2006; 235:1194–1218. [PubMed: 16502415]

Noden DM, Trainor PA. Relations and interactions between cranial mesoderm and neural crest populations. J. Anat. 2005; 207:575–601. [PubMed: 16313393]

O'Rourke JR, Georges SA, Seay HR, Tapscott SJ, McManus MT, Goldhamer DJ, Swanson MS, Harfe BD. Essential role for Dicer during skeletal muscle development. Dev. Biol. 2007; 311:359–368. [PubMed: 17936265]

Rinon A, Lazar S, Marshall H, Buchmann-Moller S, Neufeld A, Elhanany-Tamir H, Taketo MM, Sommer L, Krumlauf R, Tzahor E. Cranial neural crest cells regulate head muscle patterning and differentiation during vertebrate embryogenesis. Development. 2007; 134:3065–3075. [PubMed: 17652354]

Ryan K, Chin AJ. T-box genes and cardiac development. Birth Defects Res. C Embryo Today. 2003; 69:25–37. [PubMed: 12768655]

Ryan AS, Nicklas BJ, Berman DM, Ferrell RE. The insertion/deletion polymorphism of the ACE gene is related to insulin sensitivity in overweight women. Diabetes Care. 2001; 24:1646–1652. [PubMed: 11522714]

Saxena A, Tabin CJ. MiRNA-processing enzyme Dicer is necessary for cardiac outflow tract alignment and chamber septation. Proc. Natl. Acad. Sci. USA. 2010; 107:87–91. [PubMed: 20018673]

Snider P, Olaopa M, Firulli AB, Conway SJ. Cardiovascular development and the colonizing cardiac neural crest lineage. ScientificWorldJournal. 2007; 7:1090–1113. [PubMed: 17619792]

Stoller JZ, Epstein JA. Cardiac neural crest. Semin. Cell Dev. Biol. 2005; 16:704–715. [PubMed: 16054405]

Tzahor E, Kempf H, Mootoosamy RC, Poon AC, Abzhanov A, Tabin CJ, Dietrich S, Lassar AB. Antagonists of Wnt and BMP signaling promote the formation of vertebrate head muscle. Genes Dev. 2003; 17:3087–3099. [PubMed: 14701876]

Wang DZ. MicroRNAs in cardiac development and remodeling. Pediatr. Cardiol. 2010; 31:357–362. [PubMed: 20135107]

Wang Y, Medvid R, Melton C, Jaenisch R, Blelloch R. DGCR8 is essential for microRNA biogenesis and silencing of embryonic stem cell self-renewal. Nat. Genet. 2007; 39:380–385. [PubMed: 17259983]

Zehir A, Hua LL, Maska EL, Morikawa Y, Cserjesi P. Dicer is required for survival of differentiating neural crest cells. Dev. Biol. 2010; 340:459–467. [PubMed: 20144605]

Zhao Y, Srivastava D. A developmental view of microRNA function. Trends Biochem. Sci. 2007; 32:189–197. [PubMed: 17350266]

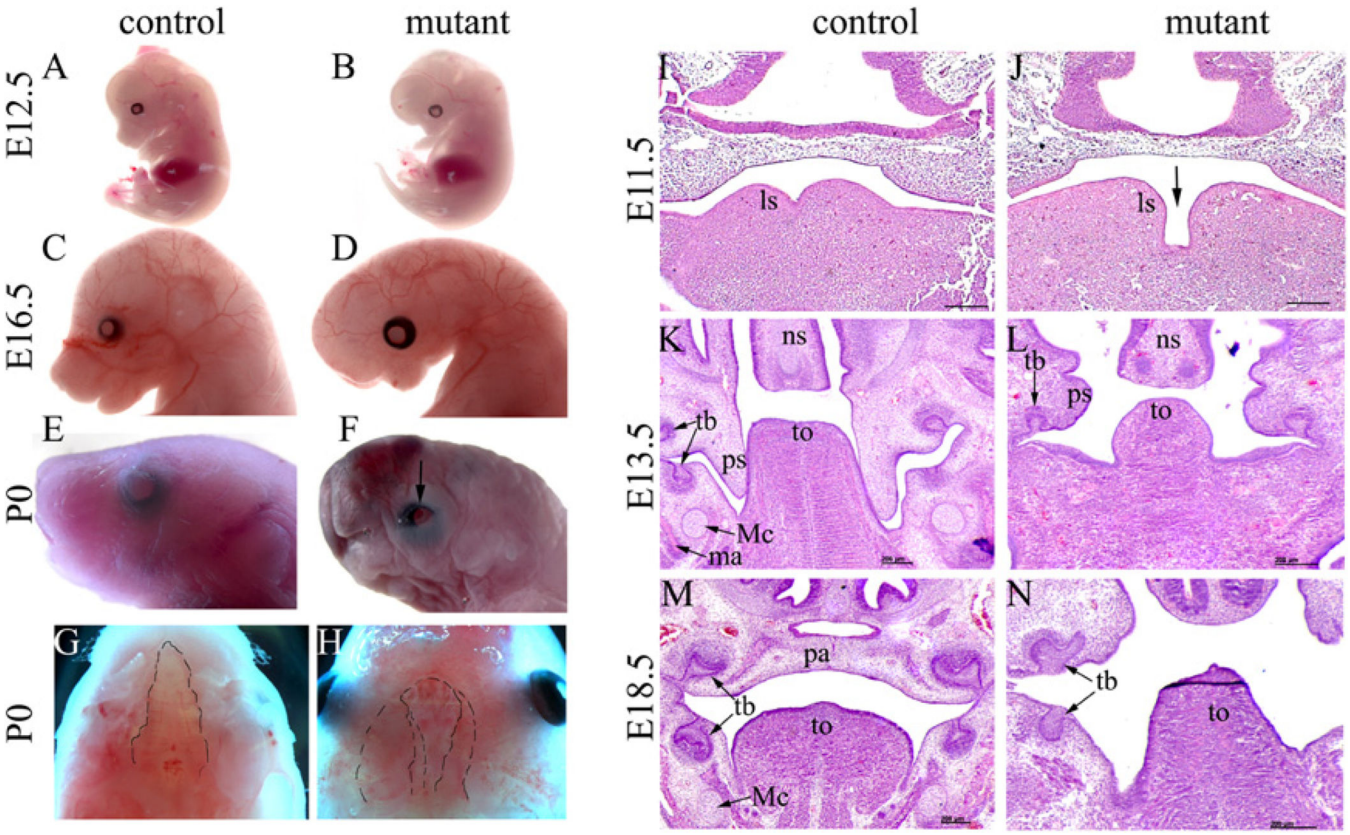

Fig. 1.

NCC-expression of *Dicer* is required for normal craniofacial morphogenesis. (**A**–**H**) The gross craniofacial structures of control (*Dicer*$^{loxP/loxP}$) and mutant (*Wnt1-Cre*; *Dicer*$^{loxP/loxP}$) mice were examined at various stages. Beginning at E12.5, mutant embryos displayed a retrognathia face and short nose (A, B), and the gross abnormality became more apparent at E16.5 (C, D). Newborn mutant embryos displayed multiple craniofacial defects, including microcephaly, hypoplasia and retrognathia face, short nose, microstomia, open eyelids (indicated by arrow), and bilateral complete cleft palate (outlined with the dotted line) (E–H). Images in Fig. 1G and H are viewed ventral-dorsally. The dotted line was drawn on the margins of the palate (control and mutant) and nasal septum (mutant) to outline the cleft condition in the mutant. (**I**–**N**) Embryos at various stages were transversely sectioned and HE stained. In mutants at E11.5, expansion of lingual swellings was reduced and they failed to merge (I, J). At E13.5, mutants displayed abnormal outgrowth of palatal shelves such that they were smaller and grew horizontally and the tongue was also smaller than that of controls (K, L). At E18.5, mutant embryos displayed bilateral complete palatal cleft and were devoid of NCC-derived Meckel's cartilage (M–N). ls, lingual swelling; ma, mandible; Mc, Meckel's cartilage; ns, nasal cartilage; pa, palate; ps, palatal shelf; tb, tooth bud; to, tongue; Scale bar: 200 μm.

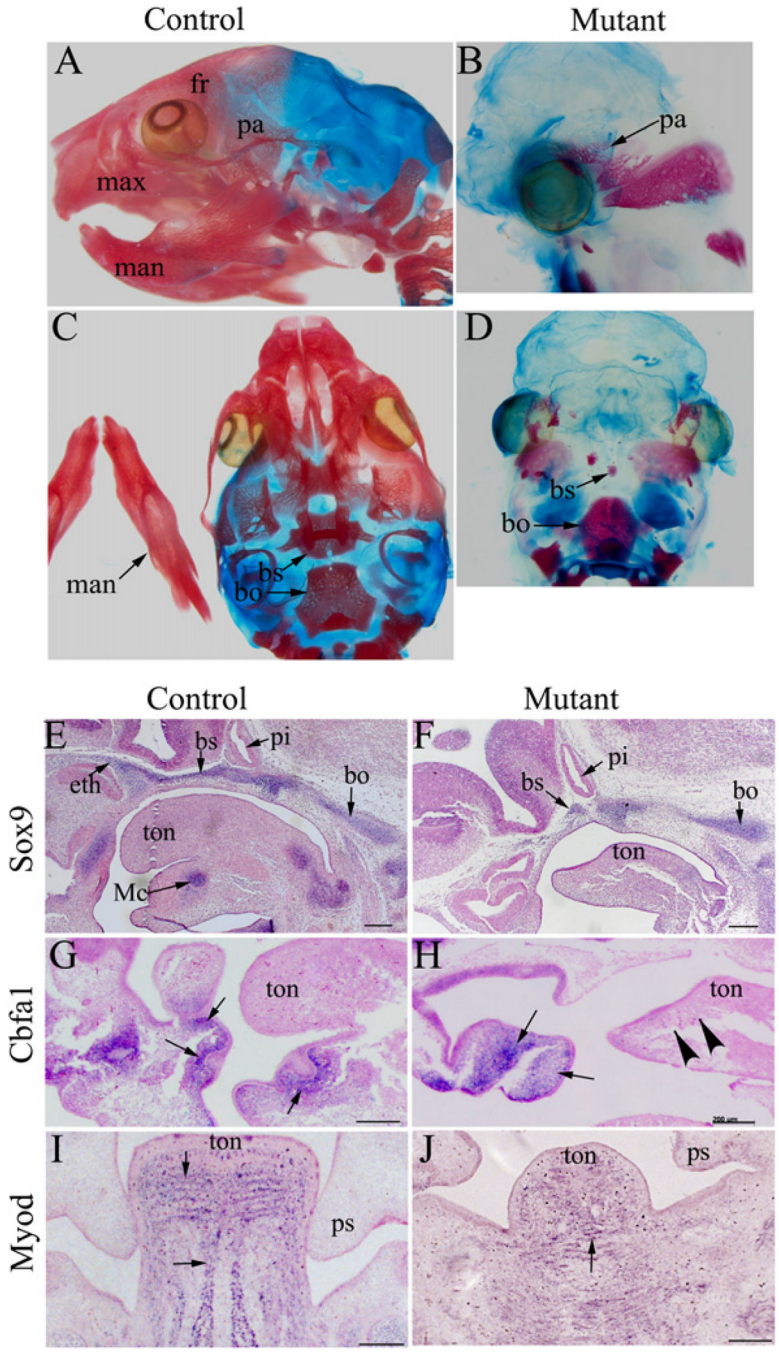

Fig. 2.

NCC-disruption of *Dicer* leads to abnormal skeletogenesis and muscle development in the craniofacial region. (**A**–**D**) Control (A, C) and mutant (B, D) head skeletons from newborn mice were stained with Alizarin red and Alcian blue. Head skeletons in the mutant mice were either missing or rudimentary. (**E**–**H**) *In situ* hybridization analysis was performed on sagittal sections of control (E, G) and mutant (F, H) embryos at E11.5 using probes against *Sox9* (E, F) and *Cbfa1* (G, H). Meckel's cartilage and anterior basicranium (labeled by *Sox9*) were absent in mutants (E, F). Osteoblasts, which express *Cbfa1*, were absent in the

mandible of mutants (indicated by arrow heads) (G, H). Arrows indicate positively stained cells. (I, J) *In situ* hybridization analysis was performed on transverse sections of control (I) and mutant (J) embryos at E13.5 using a probe against *MyoD*. In contrast to the striped pattern of muscle precursors observed in the primitive tongue of control animals, no obvious organization of muscle precursors was detected in mutant embryos. Arrows indicate examples of positively stained cells. bo, basioccipital; bs, basiosphenoid bone; eth, ethmoid bone; fr, frontal bone; man, mandible; max, maxilla; Mc, Meckel's cartilage; pa, parietal bone; pi, pituitary gland; ps, palatal shelf; ton, tongue; Scale bar: 500 μm.

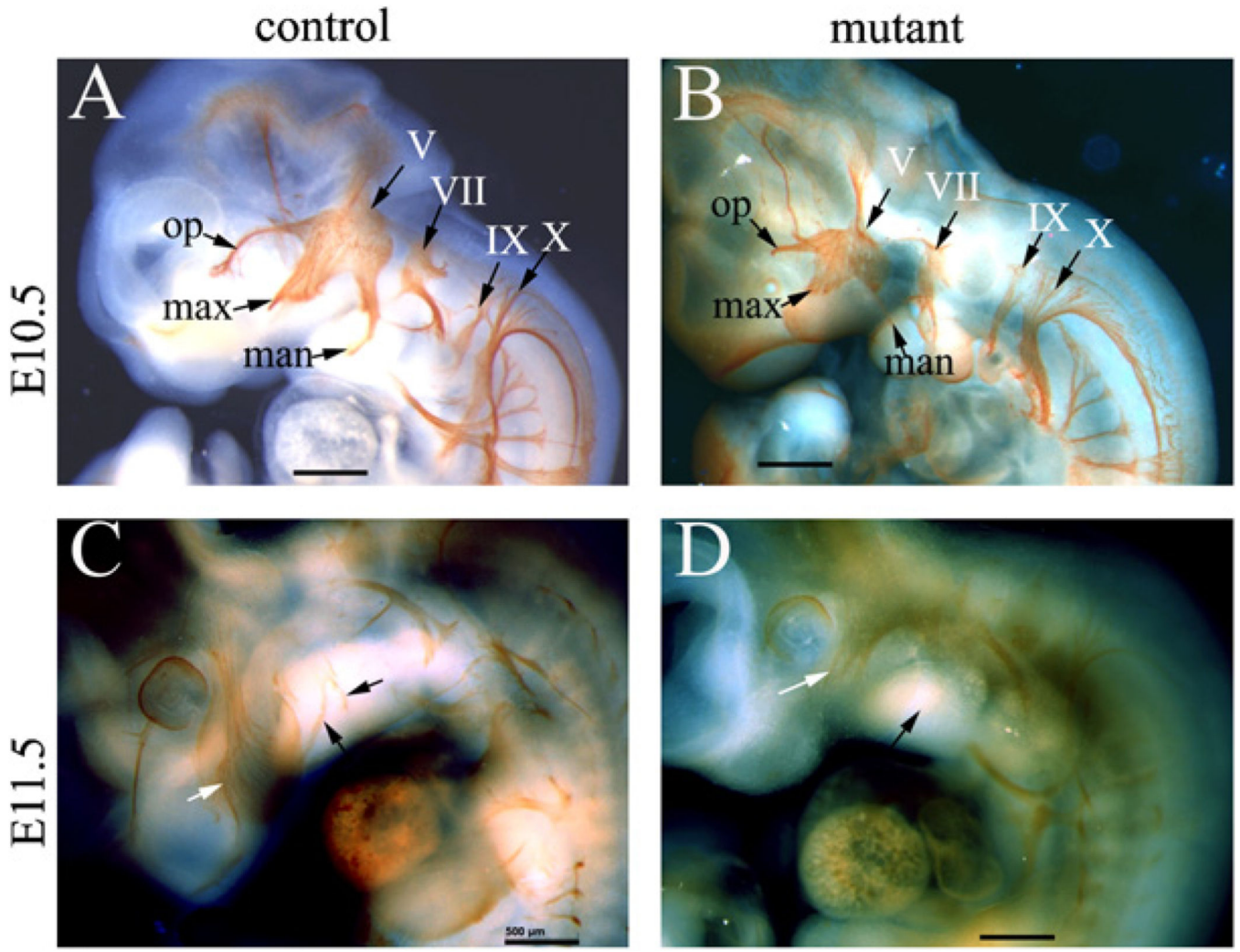

Fig. 3.

Wnt1-Cre; *Dicer*$^{loxP/loxP}$ embryos display defective morphogenesis of cranial ganglion and nerves. Whole mount immunostaining for cranial ganglia and nerves was performed using a 2H3 antibody on E10.5 (A, B) and E11.5 (C, D) embryos. Mutant embryos displayed hypoplasia trigeminal ganglia at E10.5 (A, B). The three branches from this ganglion (ophthalmic, maxillary and mandibular nerve branches) were also smaller compared to controls (**A**–**B**). In mutant embryos at E11.5, the mandibular arch was visibly devoid of neurofibers (C, D). White arrows: nerve fibers in the maxillary arches; black arrows: nerve fibers in the mandibular arch. V: the fifth cranial nerve (trigeminal nerve); VII: facial nerve; IX: glossopharyngeal nerve; X: vagus nerve; man: mandibular branch; max: maxillary branch; op: ophthalmic branch; Scale bar: 500 μm.

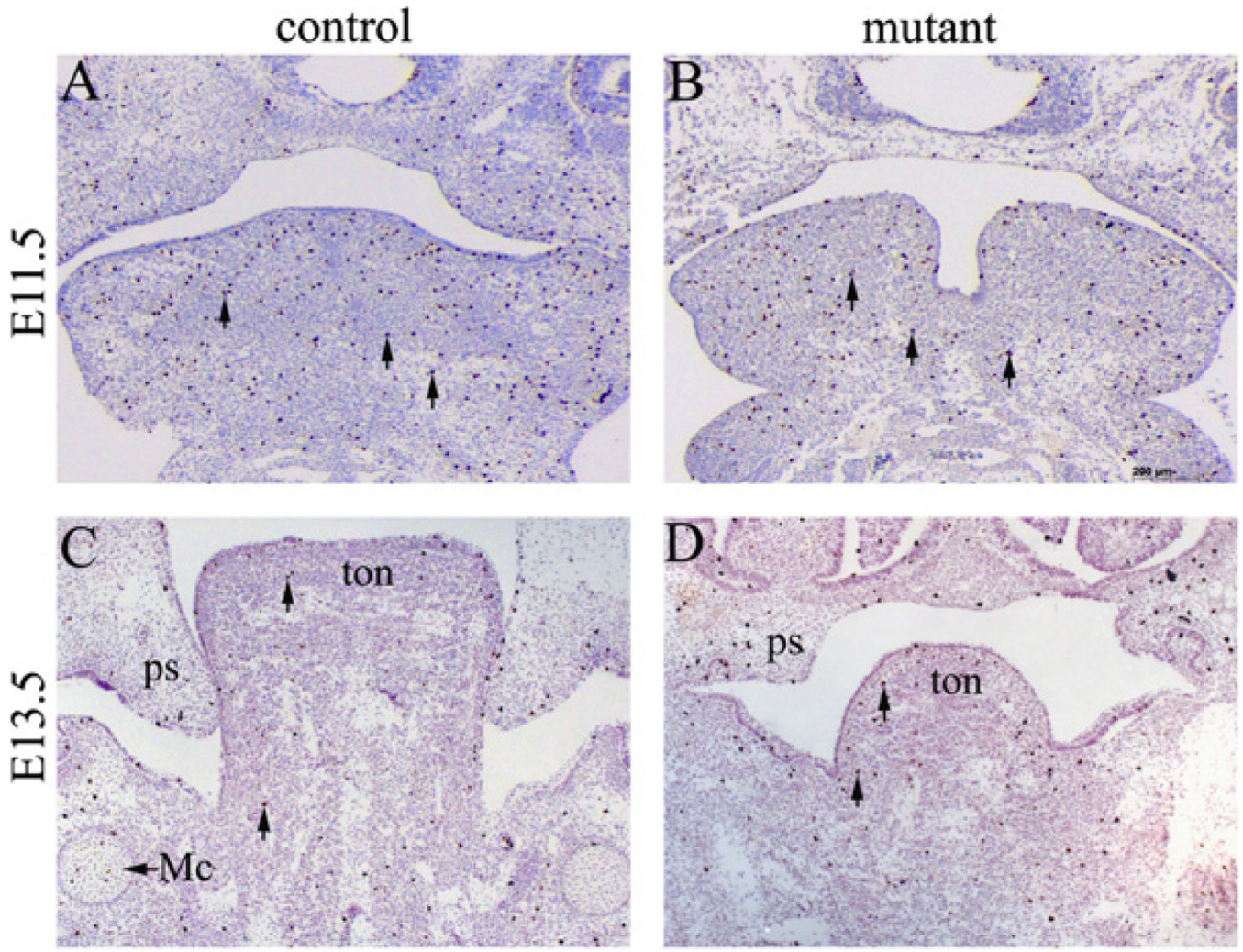

Fig. 4.

Mutant embryos show normal cell proliferation during craniofacial development. Transverse sections of control and mutant embryos at E11.5 (A, B) and E13.5 (C, D) were immunostained with an anti-phospho-Histone H3 antibody. Arrows indicate examples of positively stained cells. Cell proliferation in the mutant craniofacial area was not significantly affected. Similar results were obtained from sections obtained from other planes and at other stages (data not shown). Mc, Meckel's cartilage; ps, palatal shelf; ton, tongue; Scale bar: 200 μm.

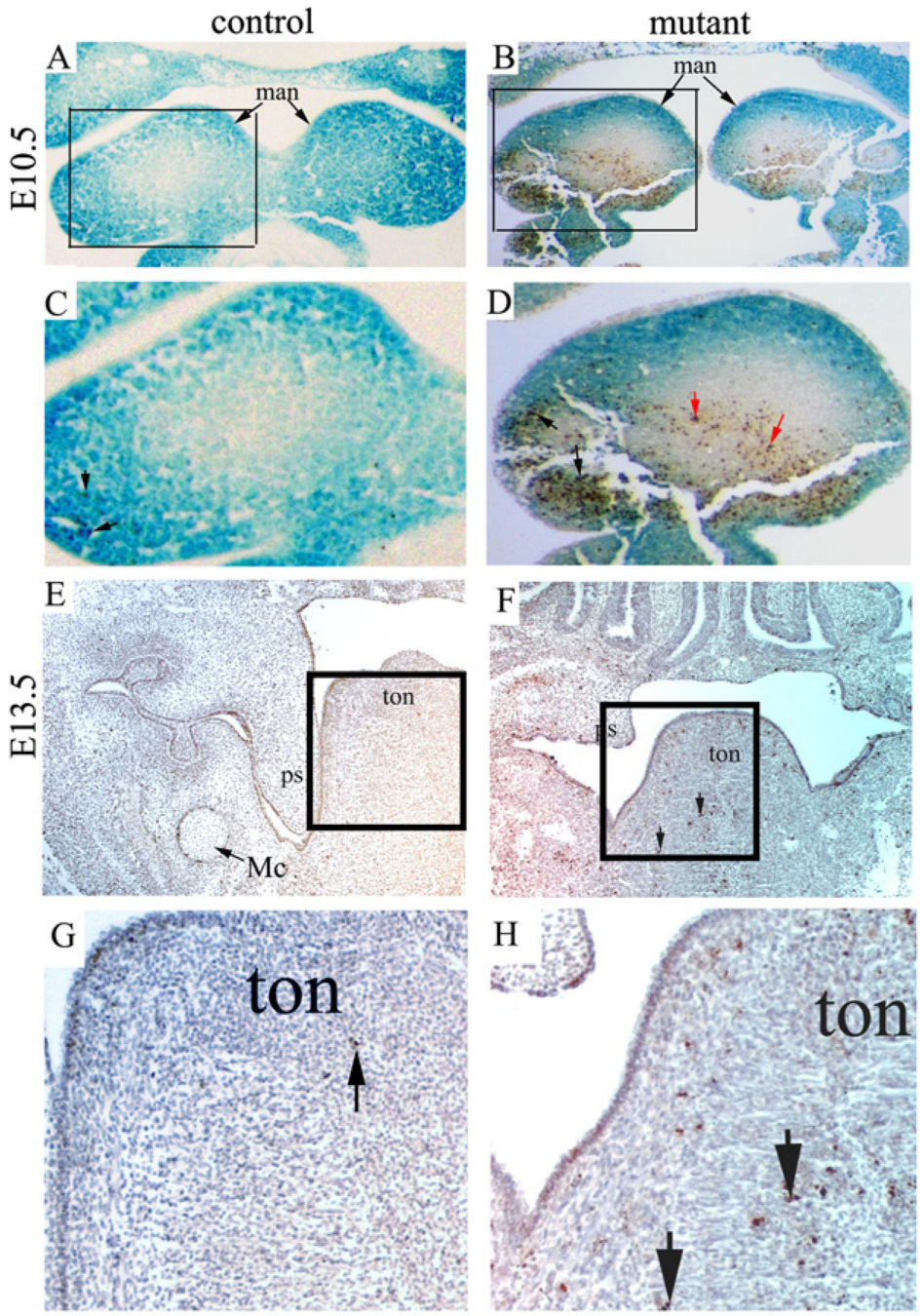

Fig. 5.

Mutant embryos display abnormal apoptosis during craniofacial development. (**A**–**D**) A mutant (*Wnt1-Cre*; *Dicer*$^{loxP/loxP}$; *R26R*) and a littermate control (*Wnt1-Cre*; *Dicer*$^{loxP/+}$; *R26R*) embryo were stained with X-gal, transversely sectioned, and subjected to TUNEL staining. LacZ positive cells are derived fromneural crest cells. Panels C and D correspond to the boxed area of panels A and B, respectively. Black arrows in panels C and D indicate examples of apoptotic cells that were also lacZ positive, while red arrows in panel D indicate examples of apoptotic cells that were lacZ negative. Increased apoptosis was

detected in both neural crest derivatives and mesodermal mesenchymal cells in the mutant. (**E**–**H**) A mutant (*Wnt1-Cre*; *Dicer*$^{loxP/loxP}$) and a littermate control (*Wnt1-Cre*; *Dicer*$^{loxP/+}$) embryo at E13.5 were transversely sectioned and subjected to TUNEL staining. Panels G and H correspond to the boxed area of panels E and F, respectively. Arrows indicate examples of positively stained cells. man, mandibular arch; Mc, Meckel's cartilage; ps, palatal shelf; ton, tongue.

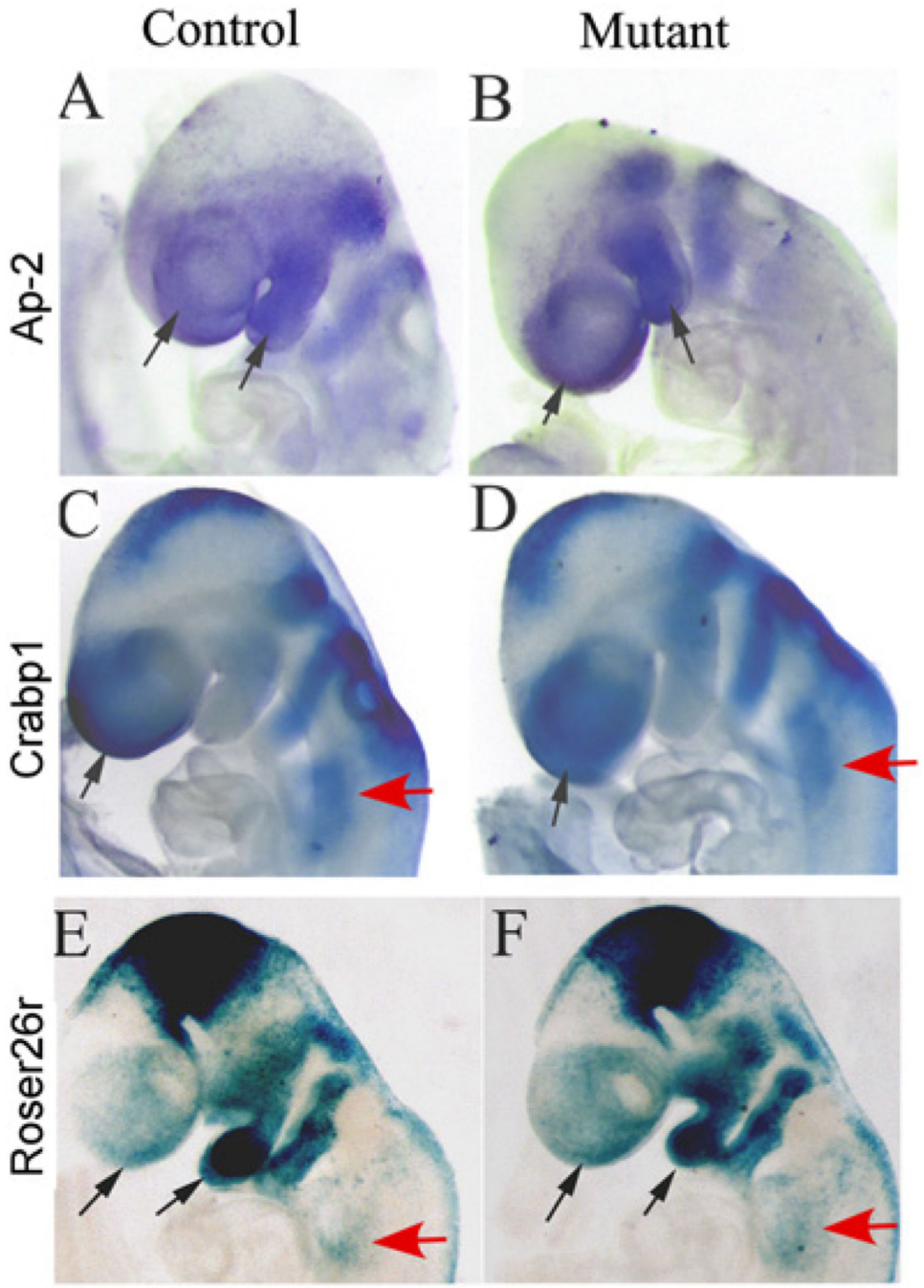

Fig. 6.

NCC migration is not affected in mutant embryos. (**A**–**D**) Whole mount *in situ* hybridization was performed on mutant (*Wnt1-Cre*; *Dicer*$^{loxP/loxP}$) and control (*Wnt1-Cre*; *Dicer*$^{loxP/+}$) embryos at E9.0 using probes against *Ap-2* (A, B) and *Crabp1* (C, D). No apparent difference in the presumptive facial (black arrows) and pharyngeal (red arrows) areas was observed between control and mutant embryos. (**E**, **F**) LacZ staining of mutant (*Wnt1-Cre*; *Dicer*$^{loxP/loxP}$; *R26R*) and control (*Wnt1-Cre*; *Dicer*$^{loxP/+}$; *R26R*) embryos at E9.0 showed

comparative distribution of NCC derivatives in the presumptive facial (black arrows) and pharyngeal (red arrows) areas.

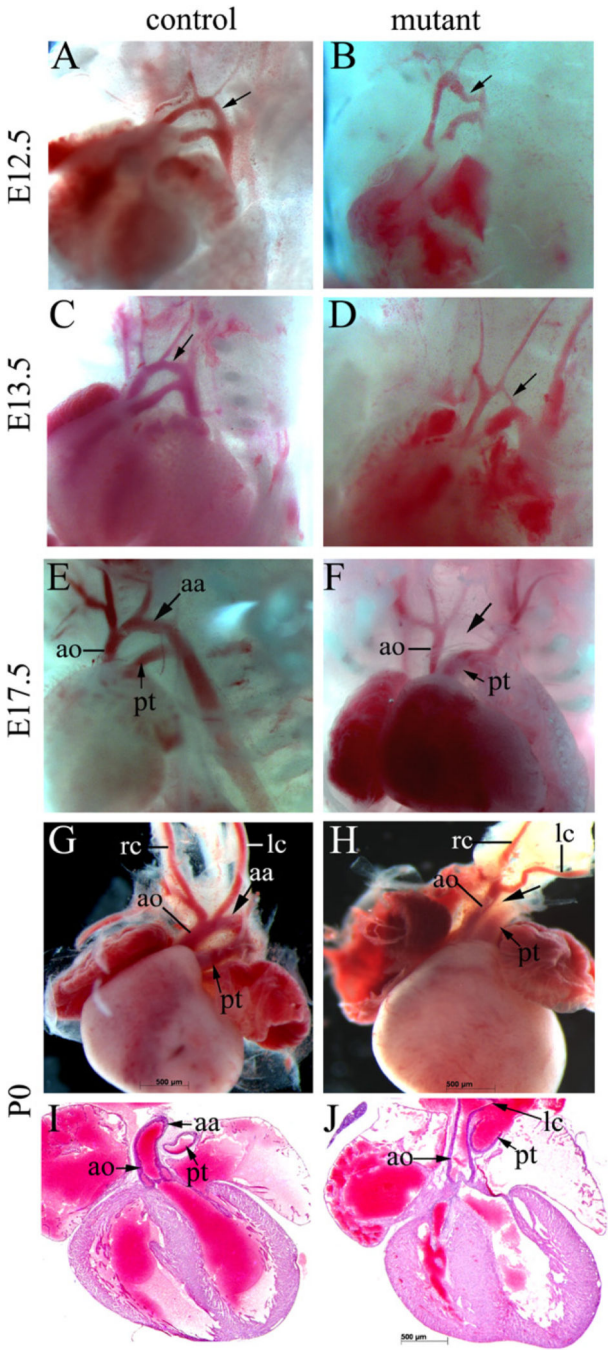

Fig. 7.

Mutant embryos display an interrupted aortic arch. (**A**–**F**) The PAA regions of mutant (*Wnt1–Cre*; *Dicer*$^{loxP/loxP}$) and control (*Wnt1-Cre*; *Dicer*$^{loxP/+}$) embryos at E12.5 (A, B), E13.5 (C, D) and E17.5 (E, F) were grossly examined. The aortic arch, which is indicated by arrows, appeared to be narrowed at E12.5 (panel B). This defect became apparent at E13.5 and by E17.5, all mutant embryos displayed IAA-B. (**G**–**J**) Hearts from mutant and control newborns were dissected for gross examination (G, H) and frontal sectioning (I, J). All mutants examined displayed IAA-B (G, H), but showed normal OFT development (I, J). aa,

aortic arch; ao, ascending aortic artery; lc, left carotid artery; pt, pulmonary trunk; rc, right carotid artery.